

# A Low-Rate Code-Spread and Chip-Interleaved Time-Hopping UWB System

Kai Li, Xiaodong Wang, *Senior Member, IEEE*, Guosen Yue, and Li Ping, *Member, IEEE*

**Abstract**—We consider a code-spread and chip-interleaved time-hopping (TH) multiple-access scheme for multiuser ultra-wideband (UWB) communications. In such a system, each user's chip sequence is interleaved by a user-specific distinct random interleaver, and the receiver is a low-complexity chip-level iterative multiuser detector (MUD) which performs simple Rake-type combining to collect the energy dispersed in multipath UWB channels. To further reduce the receiver complexity, time reversal (TR), a transmitter preprocessing technique, is also considered. When power control is employed along with TR, a single-tap receiver can be utilized which offers a desirable bit error rate (BER) performance with a significantly reduced sampling rate. Furthermore, the zigzag Hadamard (ZH) code is proposed as the low-rate code for both channel coding and spreading in the code-spread TH-UWB system. With its capacity-approaching capability and low encoding/decoding complexity, the parallel concatenated ZH code is a promising coding scheme for UWB applications.

**Index Terms**—Chip-interleaving, iterative multiuser detection, multiple access, time-hopping, time reversal (TR), ultra-wideband (UWB), zigzag Hadamard (ZH) codes.

## I. INTRODUCTION

RECENTLY, impulse radio (IR)-based [1] time-hopping (TH) ultra-wideband (UWB) technologies for short-range high-rate multiuser wireless communications have attracted significant interests [2], [3]. For a multiuser UWB system, the capability of providing high data rate with relatively low complexity and low power consumption is the key. In a typical UWB channel, due to the rich scattering environment, the number of multipath components is on the order of several hundreds, a situation that makes the collection of the widely scattered signal components a challenging task, especially when a low-complexity receiver structure is preferred. In this paper, we consider the chip-interleaved [4]–[6] multiple-access technique for multiuser UWB systems. In this scheme, each user's chip sequence is interleaved by a user-specific distinct random interleaver, and the receiver applies a low-complexity iterative multiuser detection (MUD) principle [7] at the chip

level, where a simple Rake-type combining is utilized to collect the energy dispersed in the multipath channel. To further reduce the receiver complexity, we consider the time reversal (TR) technique, which was originally employed for wideband transmission in underwater acoustics [8]–[11], ultrasound [11], [12], and spread spectrum communications [13], and was recently introduced to the field of UWB wireless communications [14] to alleviate the problem arising from a large number of multipath components. When power control is employed along with TR, a single-tap receiver can be utilized at the receiver which can offer a desirable bit error rate (BER) performance with a significantly reduced sampling rate.

In code-division multiple-access (CDMA) systems, spreading can be achieved by low-rate coding, which leads to code-spread systems [15], [16]. According to [17], low-rate code is necessary for a spectrally-efficient multiple-access system. Recently, along with the discovery of turbo codes, new low-rate concatenated codes have been proposed. In particular, it is reported in [18] that the turbo-Hadamard codes constructed from Hadamard code arrays achieve the BER of  $10^{-5}$  at  $E_b/N_0 = -1.2$  dB, which is only 0.39 dB away from the ultimate Shannon limit. Later on, another class of low-rate codes named zigzag Hadamard (ZH) codes and their concatenation schemes are proposed, where the component code is constructed by a highly structured zigzag graph [19] with each segment being a Hadamard codeword. The performance of PCZH codes is close to that of turbo Hadamard codes, whereas the former has much lower encoding and decoding complexity due to the simple zigzag graph structure. With these desirable features, PCZH codes are a promising candidate for code-spread TH-UWB multiuser systems.

The remainder of this paper is organized as follows. Section II describes the channel model, the time-reversal technique, and the chip-interleaved multiuser TH-UWB system. Section III presents the chip-level iterative detection scheme. Section IV treats the PCZH-coded system. Numerical results are presented in Section V. Section VI contains the conclusions.

## II. SYSTEM DESCRIPTIONS

### A. UWB Channel Modeling

We assume a quasi-static multipath fading channel with  $L_{\text{ch}}$  tap-coefficients for each user. The  $k$ th user's signal is transmitted through the multipath UWB channel with channel impulse response (CIR)  $h_k(t)$  given by  $h_k(t) = \sum_{l=0}^{L_{\text{ch}}-1} h_{k,l} \delta(t - \tau_l)$ , where  $h_{k,l}$  and  $\tau_l$  are, respectively, the channel coefficient and the delay of the  $l$ th component. The standardized channel model for indoor UWB environments [20] proposed by the channel modeling subcommittee of the IEEE 802.15.3a Task Group is a modified version

Manuscript received March 13, 2005; revised October 14, 2005. This work was supported in part by the U.S. National Science Foundation (NSF) under Grant CCR-0207550, and in part by the U.S. Office of Naval Research (ONR) under Grant N00014-03-1-0039.

K. Li and X. Wang are with the Department of Electrical Engineering, Columbia University, New York, NY 10027 USA (e-mail: likai@ee.columbia.edu; wangx@ee.columbia.edu).

G. Yue is with the NEC Laboratories America, Inc., Princeton, NJ 08540 USA (e-mail: yueg@nec-labs.com).

L. Ping is with the Department of Electronic Engineering, City University of Hong Kong, Kowloon, Hong Kong (e-mail: eeliping@cityu.edu.hk).

Digital Object Identifier 10.1109/JSAC.2005.863872

of the Saleh–Valenzuela (S–V) model [21], where the Rayleigh distribution of the channel coefficient amplitude in the S–V channel model is replaced by the log-normal distribution, and the phase is also constrained to take value of either 0 or  $\pi$  with equal probability which accounts for signal inversion due to reflection, resulting in a *real-valued* channel model. Such a UWB channel model is claimed to better match the measurements.

### B. Time-Reversal Scheme

For a typical UWB channel, the spacing among multipath delays is on the order of nanoseconds, and due to the rich scattering environment the number of multipath components is on the order of several hundreds, a situation that makes the collection of energy from the widely scattered signal components a challenging task, especially given a low-complexity receiver structure is preferred.

Recently, a technique called time reversal (TR), which was originally employed in wideband transmission in underwater acoustics and ultrasound, was introduced to the field of UWB communications [14] to alleviate the problem arising from the large number of multipath components in UWB channels. The basic idea is to introduce a prefilter that is a time-reversed version of CIR to the transmitter end, which will produce an equivalent channel with most of its energy concentrated on a much smaller number of multipath components and hence significantly reduce the complexity at the receiver. With CIR  $h_k(t)$ , the prefilter is  $h_k(-t)$  which yields an effective channel  $h_k^{\text{TR}}(t) \triangleq \frac{1}{\sqrt{E_{H,k}}} h_k(-t) \star h_k(t)$ , where  $\star$  denotes convolutional operation and the factor  $(1/\sqrt{E_{H,k}})$  normalizes the transmit power with  $E_{H,k} = \int |h_k(t)|^2 dt$  being the energy of the channel for the  $k$ th user. A convolution with a time-reversed signal is equivalent to an autocorrelation. For a typical UWB channel, the CIR can be viewed as a very long random code sequence like in CDMA, and the autocorrelation property of this sequence results in the time compression property of the effective TR channel, and consequently reduces the complexity at the receiver.

As shown in [14], the CIR of the effective TR channel (TR-CIR) is compressed and there is a temporal focus of energy in the center of the TR-CIR. Denote the discrete TR-CIR of the  $k$ th user as  $\{h_{k,l}^{\text{TR}}\}_l$  and its central tap index as 0. Then, we have [14]

$$h_{k,l}^{\text{TR}} = \frac{1}{2\pi\sqrt{E_{H,k}}} \int_{-\pi}^{\pi} |H_k(\omega)|^2 \exp(j\omega l) d\omega \quad (1)$$

where  $H_k(\omega)$  is the Fourier transform of  $h_k(t)$  and  $j \triangleq \sqrt{-1}$ . And the energy of the zeroth tap of the TR channel is given by  $E_{k,0}^{\text{TR}} = |h_{k,0}^{\text{TR}}|^2 = E_{H,k}$ .

Note that the proposed TR scheme in [14] normalizes the transmit power of the prefilter with the square root of the channel's energy  $E_{H,k}$ . Hence, the energy of the main peak of the TR-CIR equals the energy of the original channel. If we go a step further and perform power control (PC) at the transmitter, i.e.,

$$h_k^{\text{TR}}(t) \triangleq \frac{1}{E_{H,k}} h_k(-t) \star h_k(t) \quad (2)$$

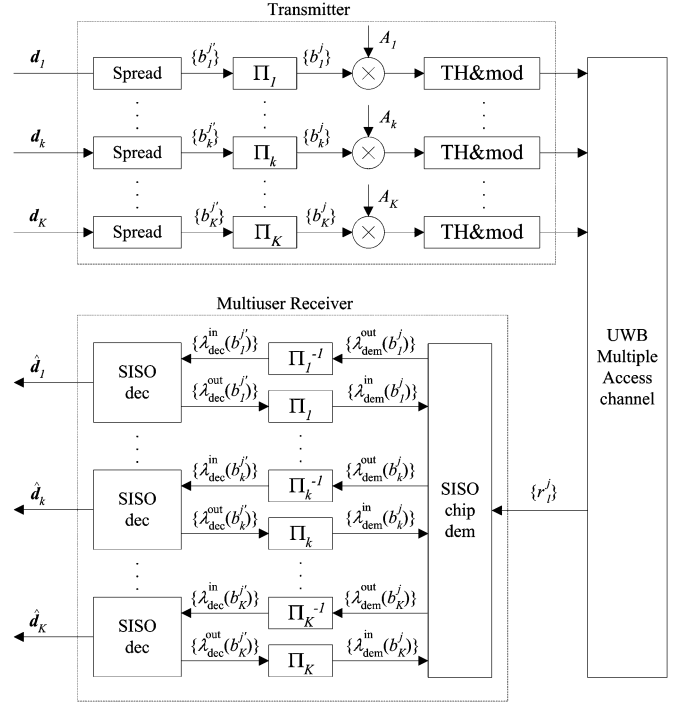


Fig. 1. Energies of a UWB channel realization and its time-reversed effective channel. Sampling interval of the channel is 1 ns.

we have  $h_{k,0}^{\text{TR}} = 1$ , which corresponds to a nonfading channel. Since the energy of the main peak is large enough, an extremely simple single-tap receiver can be utilized which can still provide desirable performance. And with a single-tap receiver, the sampling rate at the receiver can also be significantly reduced.

### C. Chip-Interleaved Time-Hopping UWB System

Here, we consider an uncoded chip-interleaved time-hopping (TH) UWB system with  $K$  users, as shown in Fig. 1. At the transmitter end, the  $n$ th information bit of the  $k$ th user  $d_k^n \in \{+1, -1\}$ ,  $n = 1, 2, \dots, N_{\text{info}}$ , in the input data stream  $\mathbf{d}_k$  is spread by a rate- $R_c$  repetition code. The chip sequence after spreading is then  $\{b_k^j\}_{j=1}^P$ , where  $P = N_{\text{info}}/R_c$  is the block length of the chips. An interleaver  $\Pi_k$  of length  $P$  is then applied to produce  $\{b_k^j\}_{j=1}^P$  which is subsequently transmitted through the channel after modulation, TH, and prefiltering. For a coded system, the rate- $R_c$  repetition code can be replaced by a low-rate channel code which yields a code-spread TH-UWB system. In Section IV, we propose to use ZH codes and their concatenated schemes for the code-spread purpose.

For clarity, here we consider only a synchronous binary pulse amplitude modulated (BPAM) system in a quasi-static TH-UWB channel. The  $k$ th user's signal in such a system before prefiltering is given by

$$x_k(t) = \sum_{j=1}^P \sum_{i=0}^{N_c-1} A_k c_k^j(i) b_k^j \omega(t - jT_f - iT_c) \quad (3)$$

where  $A_k$  is the signal amplitude;  $T_f$  and  $T_c$  are, respectively, the TH frame duration and the chip duration;  $\omega(t)$  is the transmitted pulse with unit energy, i.e.,  $\int_0^{T_f} |\omega(t)|^2 dt = 1$ ;  $N_c$  is the time-hopping spreading factor;

$\left\{ \mathbf{c}_k^j \triangleq \left[ c_k^j(0), c_k^j(1), \dots, c_k^j(N_c - 1) \right]^T \right\}_j$  is the pseudo-random time-hopping spreading sequence unique to user  $k$ . For a time-hopping system,  $\mathbf{c}_k^j$  is an  $N_c$ -dimensional indicator vector with all the entries zeros except for  $c_k^j(s_k^j) = 1$ , where  $s_k^j \in \{0, 1, \dots, N_c - 1\}$ . It is clear that such a model is equivalent to that considered in [22] and the effect of  $\mathbf{c}_k^j$  is to put  $b_k^j$  in the  $s_k^j$ th chip position in the  $j$ th TH frame. In this paper, we assume that  $\left\{ s_k^j \right\}_k$  are randomly generated with the uniform distribution and vary with index  $j$  independently.

Since every user occupies a single chip position in a TH frame, in order to avoid intersymbol interference (ISI) it is required that  $N_c T_c + \tau_{L_{\text{ch}}-1} < T_f$ , where  $\tau_{L_{\text{ch}}-1}$  is the maximum delay spread of the dense multipath channel, such that an overlap between two transmitted symbols from the same user is avoided. In the case that  $T_c > \tau_{L_{\text{ch}}-1}$ , the multiuser interference (MUI) between adjacent chip positions within the same TH frame is also avoided and the remaining MUI is due to the users whose pulses occupy the same chip position.

### III. ITERATIVE DATA DETECTION

For clarity, we first consider the case where there is no prefiltering. After matched filtering, the received discrete-time signal for the  $l$ th multipath component at the  $i$ th chip position of the  $j$ th TH frame is given by

$$r_l^j(i) = h_{k,l} A_k c_k^j(i) b_k^j + \underbrace{\sum_{k' \neq k} h_{k',l} A_{k'} c_{k'}^j(i) b_{k'}^j}_{\zeta_{k,l}^j(i)} + n_l^j(i) \quad (4)$$

where  $b_k^j \in \{+1, -1\}$ , and  $n_l^j(i)$  is the zero-mean, additive white Gaussian noise (AWGN) with double-sided power spectral density  $(N_0/2)$ .

As shown in Fig. 1, the iterative chip-wise receiver consists of a soft-input soft-output (SISO) chip demodulator and a bank of  $K$  single-user SISO decoder working in a turbo manner. The chip demodulator performs a soft chip demodulation based on the channel input and the prior information provided by the decoders. Concentrating on the  $l$ th component of the  $k$ th user, on the right-hand side (RHS) of the second equality in (4),  $\zeta_{k,l}^j(i)$  represents the sum of the multiuser interference and the additive noise with respect to this user. Each  $b_k^j$  is a random variable with mean  $\bar{b}_k^j$  and variance  $\sigma_{b_k^j}^2$  (initialized to 0 and 1, respectively) which are related to the *a priori* information of  $b_k^j$  [7]. Conditioned on the channel, we have  $\bar{r}_l^j(i) = \sum_{k'=1}^K h_{k',l} A_{k'} c_{k'}^j(i) \bar{b}_{k'}^j$  and  $\sigma_{r_l^j(i)}^2 = \sum_{k'=1}^K \left| h_{k',l} A_{k'} c_{k'}^j(i) \right|^2 \sigma_{b_{k'}^j}^2 + (N_0/2)$ . To obtain a soft value on  $b_k^j$ , as in [7],  $\zeta_{k,l}^j(i)$  in (4) is approximated by a Gaussian random variable with mean and variance, respectively, given by  $\bar{\zeta}_{k,l}^j(i) = \bar{r}_l^j(i) - h_{k,l} A_k c_k^j(i) \bar{b}_k^j$  and  $\sigma_{\zeta_{k,l}^j(i)}^2 = \sigma_{r_l^j(i)}^2 - \left| h_{k,l} A_k c_k^j(i) \right|^2 \sigma_{b_k^j}^2$ . Then, the chip demodulator computes the extrinsic log-likelihood ratio (LLR) of  $b_k^j$  for the  $l$ th component of the  $i$ th chip position as

$$\lambda_{\text{dem}}^{\text{out}}(b_k^j)_{l,i} = \frac{2h_{k,l} A_k c_k^j(i) \left( r_l^j(i) - \bar{\zeta}_{k,l}^j(i) \right)}{\sigma_{\zeta_{k,l}^j(i)}^2}. \quad (5)$$

Note that the chip demodulator is essentially a low-complexity soft-interference cancellation/matched filter (SIC-MF) detector [23]. Since the  $j$ th chip of user  $k$  only occupies the  $s_k^j$ th chip position of the  $j$ th TH frame, we only need to compute  $\left\{ \lambda_{\text{dem}}^{\text{out}}(b_k^j)_{l,s_k^j} \right\}_l$ , from which the LLR of  $b_k^j$  can be obtained by the soft Rake approach [5]

$$\lambda_{\text{dem}}^{\text{out}}(b_k^j) = \sum_{l=0}^{L_r-1} \lambda_{\text{dem}}^{\text{out}}(b_k^j)_{l,s_k^j} \quad (6)$$

where  $L_r$  is the finger number of the Rake receiver. For user  $k$ , the chip demodulator outputs  $\left\{ \lambda_{\text{dem}}^{\text{out}}(b_k^j) \right\}_j$  are de-interleaved to form  $\left\{ \lambda_{\text{dem}}^{\text{out}}(b_k^{j'}) \right\}_{j'}$  and then fed to the SISO single-user decoder as the *a priori* information.

For an uncoded system, the single-user decoder is an SISO repetition decoder. To illustrate the basic calculations, we focus on the chips related to  $d_k^1$ , the first information bit of user  $k$ . Recall that  $d_k^1$  is spread into the chip sequence  $\left\{ b_k^{j'} \right\}_{j'=1}^S$ , where  $S = 1/R_c$  is the spreading factor. Due to the interleaver,  $\left\{ \lambda_{\text{dem}}^{\text{out}}(b_k^{j'}) \right\}_{j'}$  are assumed uncorrelated. Then, based on (6), the *a posteriori* LLR output of the repetition decoder for  $d_k^1$  can be computed from  $\left\{ \lambda_{\text{dec}}^{\text{in}}(b_k^{j'}) = \lambda_{\text{dem}}^{\text{out}}(b_k^{j'}) \right\}_{j'}$  as

$$\Lambda_{\text{dec}}^{\text{out}}(d_k^1) = \sum_{j'=1}^S \lambda_{\text{dec}}^{\text{in}}(b_k^{j'}). \quad (7)$$

Then, the extrinsic LLR for the chip  $b_k^{j'}$  associated with  $d_k^1$  is given by

$$\lambda_{\text{dec}}^{\text{out}}(b_k^{j'}) = \Lambda_{\text{dec}}^{\text{out}}(d_k^1) - \lambda_{\text{dec}}^{\text{in}}(b_k^{j'}). \quad (8)$$

As shown in Fig. 1, the  $K$  single-user decoders operate in parallel and produce the extrinsic LLRs  $\left\{ \lambda_{\text{dec}}^{\text{out}}(b_k^{j'}) \right\}_{k,j'}$  which are then interleaved to form  $\left\{ \lambda_{\text{dem}}^{\text{in}}(b_k^j) = \lambda_{\text{dec}}^{\text{out}}(b_k^{j'}) \right\}_{k,j}$  and fed back to the demodulator as the *a priori* information, based on which  $\left\{ \bar{b}_k^j \right\}_j$  and  $\left\{ \sigma_{b_k^j}^2 \right\}_{k,j}$  are updated as [7]

$$\bar{b}_k^j = \tanh \left( \frac{\lambda_{\text{dem}}^{\text{in}}(b_k^j)}{2} \right) \text{ and } \sigma_{b_k^j}^2 = 1 - \left( \bar{b}_k^j \right)^2 \quad (9)$$

for  $k = 1, \dots, K$ ,  $j = 1, \dots, P$ , which in turn are used by the chip demodulator to refine its outputs during the next iteration. The above procedure is repeated for a certain number of iterations. In the last iteration, the  $k$ th repetition decoder produces hard decisions  $\hat{\mathbf{d}}_k$  in the information bits  $\mathbf{d}_k$  based on the *a posteriori* LLRs given by (7). The similar procedure can be applied to coded case. In case that the TR prefiltering is introduced at the transmitter end, the equivalent channel coefficients in (4) are  $\left\{ h_{k,l}^{\text{TR}} \right\}_k$ , and the above described receiving algorithm still applies.

It is clear that the major computations of the chip-level multi-user detector are involved in obtaining (5) where the computations of  $\bar{r}_l^j(i)$  and  $\sigma_{r_l^j(i)}^2$  require the summations over all the  $K$  users. However, the results are shared by all of the users. Also, it is clear that the complexity of the Rake approach is  $O(L_r)$  per

user per chip. Hence, the normalized complexity *per user per information bit per iteration* increases linearly with  $L_r S$  but is independent of the number of users  $K$ .

#### IV. CODE-SPREAD TH-UWB SYSTEMS

In this section, we focus on the coded TH-UWB systems. In CDMA systems, spreading can be achieved by low-rate coding, which leads to the code-spread systems [15], [16]. Inspired by this, an alternative coded TH-UWB system can be obtained from uncoded one by replacing the repetition code with a low-rate channel code. Since the complexity is a big concern for UWB applications, the recently proposed ZH codes and their concatenated schemes, which are a group of capacity-approaching low-rate codes with low encoding and decoding complexity, are a promising candidate for UWB systems.

##### A. Zigzag Hadamard Code-Spread TH-UWB Systems

For a ZH code-spread TH-UWB system considered in this section, the information bits  $\mathbf{d}_k$  of length  $N_{\text{info}}$  from user  $k$  is spread by a rate- $R_c$  PCZH encoder. After code-spreading, similar to the uncoded TH-UWB systems, the chip sequence  $\{b_{k'}^{j'}\}$  are interleaved and then transmitted to the channel after modulation and TH. In case that TR scheme is utilized, the signals are fed to the prefilter before being transmitted to the UWB channel. The low-complexity PCZH encoder is briefly illustrated as follows.

To illustrate the encoder structure, for simplicity, we consider a single-user case. As shown in Fig. 2(a), a ZH codeword is described by a highly structured zigzag graph each segment being a length- $2^r$  Hadamard code, where  $r$  is the order of the Hadamard code. At the ZH encoder, the length- $N_{\text{info}}$  data stream  $\mathbf{d}$  over  $\{+1, -1\}$  is first segmented into blocks  $\{\mathbf{d}^v\}_v$ , where  $\mathbf{d}^v = [d^v(1), d^v(2), \dots, d^v(r)]$ ,  $v = 1, 2, \dots, N_{\text{info}}/r$ . For a systematic ZH encoder, with the last parity bit of the previous coded-bit segment being the first input bit to the Hadamard encoder for the current segment, the coded bits of the  $v$ th segment are obtained by the Hadamard encoder with  $\mathbf{b}^v = \mathcal{H}(b^{v-1}(2^r - 1), d^v(1), d^v(2), \dots, d^v(r))$ , where  $\mathcal{H}(\cdot)$  denotes Hadamard encoding function [18], and the codeword  $\mathbf{b}^v = [b^v(0), b^v(1), \dots, b^v(2^r - 1)]$ , with  $b^v(0) = b^{v-1}(2^r - 1)$  being the *common bit* (black circles in the figure) that connects the current segment to the previous segment and forms the zigzag structure,  $b^v(2^{i-1}) = d^v(i)$ ,  $i = 1, 2, \dots, r$ , being the systematic bits (white circles), and all other bits being the parity bits (gray circles). Note that the first bit of the first segment can be freely assigned and is usually assumed to be  $-1$ . In case that the common bits (the first bit in each segment) are not transmitted, we obtain punctured ZH codes.

Let  $\mathbf{d} = \{d^n\}_{n=1}^{N_{\text{info}}}$ ,  $\mathbf{q} = \{q^n\}_{n=1}^{N_q}$ , and  $\mathbf{p} = \{p^n\}_{n=1}^{N_p}$  denote, respectively, the information data block, the common bits, and the parity bits of a ZH codeword, where  $N_p$  and  $N_q$  are, respectively, the number of the common bits and the parity bits. Similar to turbo codes, a systematic PCZH code is constructed by concatenating  $M$  systematic ZH codes in a parallel manner, as shown in Fig. 2(b). To avoid repeating the information bits, the systematic bits are only transmitted once, and the common bits and the parity bits from the  $m$ th component encoder are transmitted, denoted, respectively, by  $\mathbf{q}^{(m)} = \{q^n(m)\}_n$  and

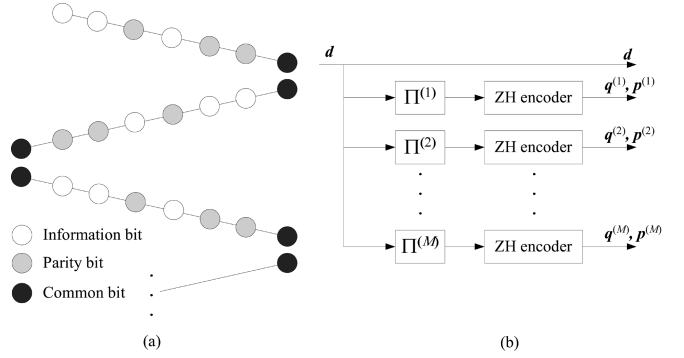


Fig. 2. (a) Graphical representation of an unpunctured systematic ZH code with  $r = 3$  (note that since the first bit of a ZH codeword is assumed to be  $-1$ , it is omitted in the graph). (b) Concatenated systematic ZH code, where  $\{\Pi^{(m)}\}$  are interleavers.

$\mathbf{p}^{(m)} = \{p^n(m)\}_n$ . Consequently, the PCZH codeword is given by  $\{\mathbf{d}, \mathbf{q}^{(1)}, \mathbf{p}^{(1)}, \dots, \mathbf{q}^{(M)}, \mathbf{p}^{(M)}\}$  and the overall code rate is given by  $R_c = (r/(r + M(2^r - r)))$ . In case that the component codes are punctured systematic ZH codes, the rate for concatenated punctured systematic codes is given by  $R_c = (r/(r + M(2^r - r - 1)))$ .

##### B. Joint Detection and Decoding of ZH Code-Spread Systems

For a PCZH code-spread TH-UWB system, the received discrete time signal after matched filtering is given by (4), with which the receiver performs chip-level joint detection as shown in Fig. 1, where now the SISO decoders are PCZH decoders.

The joint detection of a PCZH-coded multiuser UWB system comprises two iterations, i.e., the outer iteration with extrinsic information of coded bits exchanged between the chip-level demodulator and the  $K$  decoders, and the inner decoding iteration with extrinsic information of information bits exchanged between the  $M$  component ZH decoders. For the outer iteration, based on the received signal (4) and the *a priori* information of the coded bits  $\{b_{k'}^j\}_{k,j}$  from the decoders, the chip demodulator calculates the extrinsic LLRs  $\{\lambda_{\text{dem}}^{\text{out}}(b_k^j)\}_{k,j}$  as in Section III, which are then de-interleaved to form  $\{\lambda_{\text{dec}}^{\text{in}}(b_k^{j'})\}_{k,j'}$  and fed to the SISO PCZH decoders as the *a priori* information from the demodulator.

Based on  $\{\lambda_{\text{dec}}^{\text{in}}(b_k^{j'})\}_{j'}$ , the  $k$ th SISO PCZH decoder performs iterative decoding with the extrinsic information of the information bits exchanged between the  $M$  component ZH decoders. After regrouping, denote

$$\begin{aligned} & \left\{ \lambda_{\text{dec}}^{\text{in}}(b_k^{j'}) \right\}_{j'} \\ &= \left\{ \left\{ \lambda_{\text{dec}}^{\text{in}}(d_k^n) \right\}_{n=1}^{N_{\text{info}}} \left\{ \lambda_{\text{dec}}^{\text{in}}(q_k^n(1)) \right\}_{n=1}^{N_q} \right. \\ & \quad \left. \left\{ \lambda_{\text{dec}}^{\text{in}}(p_k^n(1)) \right\}_{n=1}^{N_p}, \dots, \left\{ \lambda_{\text{dec}}^{\text{in}}(q_k^n(M)) \right\}_{n=1}^{N_q} \right. \\ & \quad \left. \left\{ \lambda_{\text{dec}}^{\text{in}}(p_k^n(M)) \right\}_{n=1}^{N_p} \right\} \end{aligned} \quad (10)$$

where  $\{\lambda_{\text{dec}}^{\text{in}}(d_k^n)\}_n$  are the LLRs for the  $k$ th user's information bits  $\mathbf{d}_k$  from the demodulator;  $\{\lambda_{\text{dec}}^{\text{in}}(q_k^n(m))\}_n$  and  $\{\lambda_{\text{dec}}^{\text{in}}(p_k^n(m))\}_n$  are, respectively, the LLRs for the common

bits  $q_k^m$  and the parity bits  $p_k^m$  associated with the  $m$ th component ZH code. Similar to the message-passing scheduling of turbo codes, at the  $m$ th decoding stage, the  $m$ th ZH decoder computes the *a posteriori* LLR value of the  $n$ th information bit with (11), shown at the bottom of the page, where  $\{\lambda_{\text{zh}}^{m-1}(d_k^n)\}_n$  are the extrinsic LLRs of the information bits passing from the  $(m-1)$ th ZH decoder. Note that we have  $\{\lambda_{\text{zh}}^{m=0}(d_k^n) = \lambda_{\text{zh}}^M(d_k^n)\}_n$  and for the first iteration they are initialized to zeros. Since the encoding of a ZH code is a Markov process, the computation of (11) is similar to that of the zigzag code [19] which is a low-complexity two-way algorithm. The only difference is that the component decoder of a ZH code for each segment is an *a posteriori* probability (APP) Hadamard decoder, and the APP Hadamard decoding can be implemented by efficient fast Hadamard transform (FHT) and APP-FHT [18]. With (11), the extrinsic LLR of  $d_k^n$  that the  $m$ th ZH decoder produces is given by

$$\begin{aligned} \lambda_{\text{zh}}^m(d_k^n) &= \Lambda_{\text{zh}}^m(d_k^n) - \ln \frac{\Pr(d_k^n = +1)}{\Pr(d_k^n = -1)} \\ &= \Lambda_{\text{zh}}^m(d_k^n) - (\lambda_{\text{zh}}^{m-1}(d_k^n) + \lambda_{\text{dec}}^{\text{in}}(d_k^n)) \end{aligned} \quad (12)$$

which will be used for the next stage ZH decoding, as shown in (11). After several inner decoding iterations, the inner iteration is temporarily interrupted after the PCZH decoder computes the extrinsic LLRs of the coded bits for the demodulator as follows:

$$\lambda_{\text{dec}}^{\text{out}}(q_k^n(m)) = \Lambda_{\text{zh}}(q_k^n(m)) - \lambda_{\text{dec}}^{\text{in}}(q_k^n(m)) \quad \text{for } n = 1, 2, \dots, N_q \quad m = 1, 2, \dots, M \quad (13)$$

$$\lambda_{\text{dec}}^{\text{out}}(p_k^n(m)) = \Lambda_{\text{zh}}(p_k^n(m)) - \lambda_{\text{dec}}^{\text{in}}(p_k^n(m)) \quad \text{for } n = 1, 2, \dots, N_p \quad m = 1, 2, \dots, M \quad (14)$$

$$\begin{aligned} \lambda_{\text{dec}}^{\text{out}}(d_k^n) &= \Lambda_{\text{zh}}^M(d_k^n) - \lambda_{\text{dec}}^{\text{in}}(d_k^n) \\ &\quad \text{for } n = 1, 2, \dots, N_{\text{info}} \end{aligned} \quad (15)$$

where  $\{\Lambda_{\text{zh}}(q_k^n(m))\}_n$  and  $\{\Lambda_{\text{zh}}(p_k^n(m))\}_n$  are, respectively, the output *a posteriori* LLRs of the  $m$ th ZH decoder for the common bits and the parity bits whose computations are similar to (11), and hence can be efficiently implemented by FHT and APP-FHT. The output extrinsic LLRs of the  $K$  single-user PCZH decoders  $\{\lambda_{\text{dec}}^{\text{out}}(b_k^{j'})\}_{k,j'} = \{\{\lambda_{\text{dec}}^{\text{out}}(d_k^n)\}_n, \{\lambda_{\text{dec}}^{\text{out}}(q_k^n(1))\}_n, \{\lambda_{\text{dec}}^{\text{out}}(p_k^n(1))\}_n, \dots, \{\lambda_{\text{dec}}^{\text{out}}(q_k^n(m))\}_n, \{\lambda_{\text{dec}}^{\text{out}}(p_k^n(m))\}_n\}_{k,j'}$  are then interleaved and fed to the demodulator as the *a priori* LLRs to update  $\{\lambda_{\text{dem}}^{\text{out}}(b_k^j)\}_{k,j}$  as in Section III. The latest  $\{\lambda_{\text{dem}}^{\text{out}}(b_k^j)\}_{k,j}$  are then de-interleaved and fed to the PCZH decoders to continue the inner decoding iterations until the next epoch for outer iteration arrives. After several outer iterations and inner iterations, the  $k$ th PCZH decoder produces hard decisions  $\hat{d}_k$  based on the output *a posteriori* LLRs of the information bits, which are given by  $\{\Lambda_{\text{dec}}^{\text{out}}(d_k^n) = \Lambda_{\text{zh}}^M(d_k^n)\}_{n=1}^{N_{\text{info}}}$ , where  $\Lambda_{\text{zh}}^M(d_k^n)$  is given by (11) with  $m = M$ .

## V. NUMERICAL RESULTS

In this section, we present simulation results to demonstrate the performance of the proposed uncoded and PCZH code-spread chip-interleaved TH-UWB system with iterative multiuser detection. The discrete time channel model proposed by the IEEE 802.15.3a working group [20] is utilized, which is based on the modified S-V model. We focus on the non-line-of-sight (NLOS) channel model 2 (CM2) in [20], which corresponds to a short-range (0–4 m) indoor wireless environment. 1000 realizations of this stochastic channel model are generated by the MATLAB code provided in [20], leading to a channel model with mean delay spread of 9.2 ns and root mean square delay of 8 ns. The simulation results are averaged over a large number of channel realizations. For the discrete time model, the minimum sampling interval of the channel is 1 ns.

### A. Uncoded Case

1) *Without TR*: We first consider the average BER performance of an uncoded chip-interleaved TH-UWB system without TR, as shown in Fig. 3. For the simulations,  $\tau_{L_{\text{ch}}-1} = 99$  ns, and  $T_c = 100$  ns, hence there is no multiuser interference between adjacent chip positions. We also assume that  $N_c T_c + \tau_{L_{\text{ch}}-1} < T_f$ , such that an overlap between two transmitted symbols from the same user is avoided. The rate of the repetition code  $R_c = 1/8$ , and the number of TH chips per TH-frame  $N_c = 4$ , which result in a total bandwidth expansion factor [24] of  $\Omega \triangleq N_c/R_c = 32$  and a basic transmission rate of around 250 Kb/s per stream. Note that higher rates can be achieved by using multistream transmission for each user.

The BER curves of such an equal-power system with different configurations of Rake receiver and perfect channel side information (CSI) at the receiver are shown in Fig. 3 where the information block length  $N_{\text{info}} = 256$ . The curve marked “single AWGN” is the single-user performance in a nonfading AWGN channel. It is seen from the figure that the BER performance with  $K = 32$  approaches the single-user performance, where the number of fingers of the Rake receiver  $L_r$  equals to the number of multipath components of the fading channel  $L_{\text{ch}}$  (the *full Rake* configuration). This shows that the chip-level iterative multiuser detector with Rake combining can effectively mitigate the MUI and collect the energy dispersed in the multipath components. It is clear that in order to collect enough energy dispersed in the multipath components, a Rake receiver with sufficient large number of fingers should be utilized. As shown in Fig. 3, with  $L_{sr} = 40$ , the Rake receiver is able to capture a large portion of the dispersed energy and yields a BER performance very close to that of the full Rake configuration. With 30-finger Rake, around 0.7-dB loss is observed when compared to the full Rake case measured at  $P_b = 10^{-5}$ , and the performances of 20- and 10-finger Rake are far away from that of the full Rake case, which is as expected. When measured at  $P_b = 10^{-2}$ , there is a loss of 1 dB for 20-finger Rake and more than 10 dB for

$$\Lambda_{\text{zh}}^m(d_k^n) = \ln \frac{\Pr(d_k^n = +1 | \{\lambda_{\text{dec}}^{\text{in}}(d_k^n)\}_n, \{\lambda_{\text{dec}}^{\text{in}}(q_k^n(m))\}_n, \{\lambda_{\text{dec}}^{\text{in}}(p_k^n(m))\}_n, \{\lambda_{\text{zh}}^{m-1}(d_k^n)\}_n)}{\Pr(d_k^n = -1 | \{\lambda_{\text{dec}}^{\text{in}}(d_k^n)\}_n, \{\lambda_{\text{dec}}^{\text{in}}(q_k^n(m))\}_n, \{\lambda_{\text{dec}}^{\text{in}}(p_k^n(m))\}_n, \{\lambda_{\text{zh}}^{m-1}(d_k^n)\}_n)} \quad (11)$$

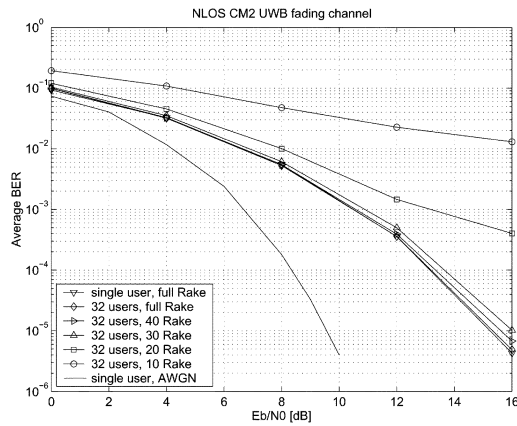


Fig. 3. BER performance of equal-power uncoded chip-interleaved TH-UWB system with different configurations of the Rake receiver.  $R_c = 1/S = 1/8$ ,  $N_c = 4$ ,  $K = 32$ ,  $N_{\text{info}} = 256$ , four iterations and with perfect CSI at the receiver.

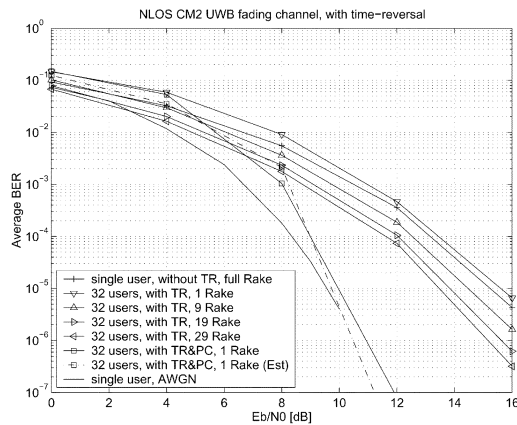


Fig. 4. BER performance of equal-power uncoded chip-interleaved TH-UWB system with time-reversal and different configurations of the Rake receiver.  $R_c = 1/S = 1/8$ ,  $N_c = 4$ ,  $K = 32$ ,  $N_{\text{info}} = 256$ , with perfect CSI at the receiver. Four iterations for the simulations.

10-finger Rake. The performance loss is even larger for lower BER, as shown in Fig. 3.

2) *With TR*: Next, we consider the BER performance of the above system with TR scheme. In the simulation,  $T_c = 99$  ns, and the maximum delay of the equivalent TR channel is  $\tau_{L_{\text{ch}}^{\text{TR}}-1} = 198$  ns, where  $L_{\text{ch}}^{\text{TR}}$  is the number of multipath components of the TR channel.

Fig. 4 shows the BER performance of the equal-power uncoded chip-interleaved TH-UWB system with time-reversal technique for  $K = 32$ , where the rate of repetition code is  $1/8$ , the number of TH chips per TH-frame  $N_c = 4$ , and the information block length  $N_{\text{info}} = 256$ . The advantage of the TR scheme is evident in the figure. With a single-tap receiver, the BER performance of the TR system is close to that of the single user bound with full Rake without TR after only four iterations. With 9-finger Rake, a gain of around 1 dB measured at  $P_b = 10^{-5}$  is observed when compared to the single-tap TR scheme, and further SNR gain can be obtained by increasing the number of fingers of the Rake receiver. When the power-controlled TR scheme (2) is utilized, the performance of single-tap receiver has a gain of around 5.5 dB measured at  $P_b = 10^{-5}$

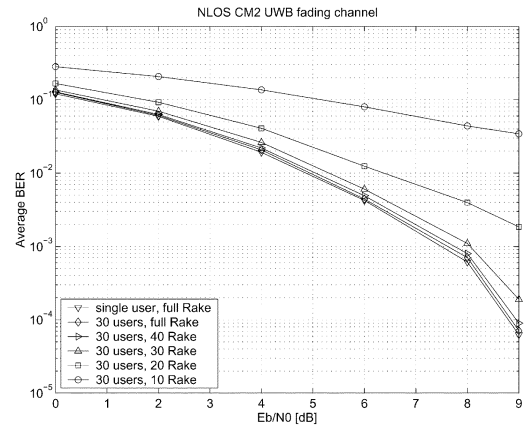


Fig. 5. BER performance of equal-power ZH-coded chip-interleaved TH-UWB system with different configurations of the Rake receiver.  $R_c \approx 0.108$ ,  $N_c = 3$ ,  $K = 30$ ,  $N_{\text{info}} = 256$ , and with perfect CSI. One iteration between the demodulator and the decoders.

when compared to that of the case of TR without power control and can approach the single-user bound in AWGN channel.

### B. Coded Case

Now we consider the BER performance of a ZH-coded chip-interleaved TH-UWB system with and without TR scheme. A punctured parallel concatenated ZH code with  $r = 6$  and  $M = 3$  is used, which leads to a coding rate of  $R_c \approx 0.108$ . The information length  $N_{\text{info}} = 256$ , and random interleavers with length- $N_{\text{info}}$  for the codes are assumed. The maximum iteration number of the ZH decoder is 30.

1) *Without TR*: We first consider the BER performance of an equal-power system without TR. The same channel parameters as the uncoded case are used. The number of TH chips per TH-frame  $N_c = 3$ , which results in a total bandwidth expansion factor of  $\Omega = N_c/R_c \approx 28$  and a transmission rate of around 250 Kb/s per stream.

The BER curves of an equal-power system for  $K = 30$  with different configurations of Rake receiver and perfect CSI at the receiver are shown in Fig. 5. Similar to the uncoded case in Fig. 4, it is seen from Fig. 5 that the BER performance of the full Rake receiver approaches the single-user bound (with a maximum iteration number of 30) with only one iteration between the decoders and the chip-level demodulator. A 40-finger Rake receiver is able to capture a large portion of the dispersed energy and yields a BER performance very close to that of the full Rake configuration. With 30-finger Rake, around 1-dB loss is observed when compared to the full Rake case measured at  $P_b = 10^{-4}$ , and the performances of 20- and 10-finger Rake are very bad, which is similar to that of the uncoded case.

2) *With TR*: Fig. 6 shows the BER performance of the equal-power ZH-coded chip-interleaved TH-UWB system with TR technique where the number of TH chips per TH-frame  $N_c = 3$ . It is seen from the figure that with the single-tap receiver, the BER performance of the TR system with  $K = 30$  and a maximum of five iterations between the demodulator and the decoders is close to that of the single-user bound with full Rake without TR. With 9-finger Rake, a gain of around 1 dB measured at  $P_b = 10^{-4}$  is observed when compared to the single-tap TR scheme, and further SNR gain can be obtained by increasing the number of fingers of the Rake receiver.

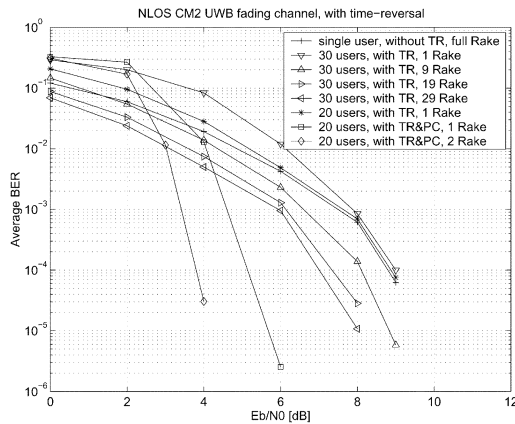


Fig. 6. BER performance of equal-power ZH-coded chip-interleaved TH-UWB system with TR and different configurations of Rake receiver.  $R_c \approx 0.108$ ,  $N_c = 3$ ,  $N_{\text{info}} = 256$ , and with perfect CSI. Five iterations between the demodulator and the decoders.

Next, we consider an equal-power system with  $K = 20$  and employing power-controlled TR scheme (2). The performance of the single-tap receiver has a gain of around 4 dB measured at  $P_b = 10^{-4}$  when compared to that of the case of TR without power control. By adding another finger, an extra 1 dB gain can be obtained, resulting to 5-dB gain when compared to the single user bound with full Rake configuration without TR, which shows the advantage of the TR scheme with power control. Note that as shown in [6], for  $K > \Omega$  which corresponds to an overloaded system, unequal power allocation should be utilized, and the optimal power profile can be obtained by using differential evolution [25].

## VI. CONCLUSION

We have proposed a new TH-UWB communication system based on chip-level random interleaving, iterative multiuser detection, and low-rate ZH coding. With chip-level interleaving, a simple iterative joint detection scheme can be utilized to effectively mitigate the multiuser interference. With TR, the equivalent channel dispersion is significantly reduced, which simplifies the complexity of the multiuser detection. When power control is employed along with TR, a single-tap Rake receiver can be utilized without channel estimation at the receiver. The latest discovery in coding area is also considered. With its capacity approaching capability and low encoding/decoding complexity, the low-rate parallel concatenated ZH code is introduced as a promising coding scheme for code-spread TH-UWB applications.

## REFERENCES

- [1] P. Wintherton II and L. W. Fullerton, "An impulse radio communications system," in *Proc. Int. Conf. Ultra-Wide Band, Short-Pulse Electromagnetics*, Brooklyn, NY, Oct. 1992, pp. 113–120.
- [2] R. A. Scholtz, "Multiple access with time-hopping impulse modulation," in *Proc. MILCOM Conf.*, Boston, MA, 1993, pp. 447–450.
- [3] M. Z. Win and R. A. Scholtz, "Ultra-wide bandwidth time-hopping spread-spectrum impulse radio for wireless multiple-access communications," *IEEE Trans. Commun.*, vol. 48, no. 4, pp. 679–691, Apr. 2000.
- [4] R. H. Mahadevappa and J. G. Proakis, "Mitigating multiple access interference and intersymbol interference in uncoded CDMA systems with chip-level interleaving," *IEEE Trans. Wireless Commun.*, vol. 1, no. 4, pp. 781–792, Oct. 2002.

- [5] L. Ping, L. Liu, K. Wu, and W. K. Leung, "Interleave division multiple access (IDMA) communication systems," in *Proc. 3rd Int. Symp. Turbo Codes Related Topics*, Brest, France, Sep. 2003, pp. 173–180.
- [6] K. Li, L. Ping, and X. Wang, "Analysis and optimization of interleave-division multiple-access communication systems," in *Proc. IEEE Int. Conf. Acoustics, Speech, Signal Process.*, vol. 3, Philadelphia, PA, Mar. 18–23, 2005, pp. 917–920.
- [7] X. Wang and H. V. Poor, "Iterative (turbo) soft interference cancellation and decoding for coded CDMA," *IEEE Trans. Commun.*, vol. 46, no. 7, pp. 1046–1061, Jul. 1999.
- [8] D. Rouseff, D. R. Jackson, W. L. J. Fox, C. D. Jones, J. A. Ritcey, and D. R. Dowling, "Underwater acoustic communication by passive-phase conjugation: Theory and experimental results," *IEEE J. Ocean. Eng.*, vol. 26, no. 4, pp. 821–831, Oct. 2001.
- [9] M. G. Heinemann, A. Larazza, and K. B. Smith, "Acoustic communications in an enclosure using single-channel time-reversal acoustics," *Appl. Phys. Lett.*, vol. 80, pp. 694–696, 2002.
- [10] G. F. Edelmann, T. Akal, W. S. Hodgkiss, S. Kim, W. A. Kuperman, and H. C. Song, "An initial demonstration of underwater acoustic communication using time reversal," *IEEE J. Ocean. Eng.*, vol. 27, no. 3, pp. 602–609, Jul. 2002.
- [11] A. Derode *et al.*, "Taking advantage of multiple scattering to communicate with time-reversal antennas," *Phys. Rev. Lett.*, vol. 90, 2003.
- [12] A. Derode, P. Roux, and M. Fink, "Robust acoustic time reversal with high-order multiple scattering," *Phys. Rev. Lett.*, vol. 75, pp. 4206–4209, 1995.
- [13] R. Esmailzadeh, E. Sourour, and M. Nakagawa, "Prerake diversity combining in time-division duplex CDMA mobile communications," *IEEE Trans. Veh. Technol.*, vol. 48, no. 3, pp. 795–801, May 1999.
- [14] T. Strohmer, M. Emami, J. Hansen, G. Papanicolaou, and A. J. Paulraj, "Application of time-reversal with MMSE equalizer to UWB communications," in *Proc. IEEE Global Telecommun. Conf.*, vol. 5, Dallas, TX, Dec. 2004, pp. 3123–3127.
- [15] A. J. Viterbi, "Very low rate convolutional codes for maximum theoretical performance of spread spectrum multiple-access channels," *IEEE J. Sel. Areas Commun.*, vol. 8, no. 6, pp. 641–649, Aug. 1990.
- [16] P. Frenger, P. Orten, and T. Ottosson, "Code-spread CDMA using maximum free distance low-rate convolutional codes," *IEEE Trans. Commun.*, vol. 48, no. 1, pp. 135–144, Jan. 2000.
- [17] S. Verdú and S. Shamai, "Spectral efficiency of CDMA with random spreading," *IEEE Trans. Inf. Theory*, vol. 45, no. 3, pp. 622–640, Mar. 1999.
- [18] L. Ping, W. K. Leung, and K. Y. Wu, "Low-rate turbo-Hadamard codes," *IEEE Trans. Inf. Theory*, vol. 49, no. 12, pp. 3213–3224, Dec. 2003.
- [19] L. Ping, X. Huang, and N. Phamdo, "Zigzag codes and concatenated zigzag codes," *IEEE Trans. Inf. Theory*, vol. 47, no. 2, pp. 800–807, Feb. 2001.
- [20] *IEEE P802.15 Wireless Personal Area Networks, P802.15-02/490r1-SG3a*, Feb. 2003.
- [21] A. A. M. Saleh and R. A. Valenzuela, "A statistical model for indoor multipath propagation," *IEEE J. Sel. Areas Commun.*, vol. 5, no. 2, pp. 128–137, Feb. 1987.
- [22] E. Fishler and H. V. Poor, "Low-complexity multiuser detectors for time-hopping impulse-radio systems," *IEEE Trans. Signal Process.*, vol. 52, no. 9, pp. 2561–2571, Sep. 2004.
- [23] K. Li and X. Wang, "EXIT chart analysis of turbo multiuser detection," *IEEE Trans. Wireless Commun.*, vol. 4, no. 1, pp. 300–301, Jan. 2005.
- [24] V. V. Veeravalli and A. Mantravadi, "The coding–spreading tradeoff in CDMA systems," *IEEE J. Sel. Areas Commun.*, vol. 20, no. 2, pp. 396–408, Feb. 2002.
- [25] K. Price and R. Storn, "Differential evolution—A simple and efficient heuristic for global optimization over continuous spaces," *J. Global Optimization*, vol. 11, pp. 341–359, 1997.

**Kai Li**, photograph and biography not available at the time of publication.

**Xiaodong Wang** (S'98–M'98–SM'04), photograph and biography not available at the time of publication.

**Guosen Yue**, photograph and biography not available at the time of publication.

**Li Ping** (S'87–M'91), photograph and biography not available at the time of publication.